The Impact of Stirring on the Electrode Microenvironment During eCO$_2$ Reduction

Katharina Trapp

Lukatskaya Research Group, Electrochemical Energy Systems Laboratory
Department of Mechanical and Process Engineering, ETH Zurich, 8092 Zurich, Switzerland

Introduction

Electrochemical CO$_2$ reduction (eCO$_2$R) is a promising pathway for producing essential chemical building blocks (e.g. CO, ethylene, or formate) using renewable energy sources. However, its industrial applicability remains limited by high overpotentials and low faradaic efficiencies for desirable products. These challenges drive ongoing research efforts to enhance catalyst performance, reaction conditions, and process efficiency [1, 2]. Surface-enhanced FTIR spectroscopy is an important spectroscopic technique to analyze, for example, reaction mechanisms, adsorbates, and electrolyte effects in eCO$_2$R. The reaction rate and selectivity significantly depend on the cell geometry and process conditions, leading to notable differences when cell variables are altered [3]. Herein, we use the Jackfish J4 H-cell to demonstrate the significant impact of stirring on the surface microenvironment of gold electrodes during eCO$_2$R.

Experimental Details

A SEIRAS-active gold coating was prepared on a face-angled Si crystal (PIKE Technologies) through a previously established electroless gold deposition procedure [4, 5]. The as-prepared gold thin films had a resistance $< 20\,\Omega$. The Jackfish H-Cell was equipped with a graphite rod and an Ag/AgCl electrode, which were used as the counter and reference electrodes, respectively. The two-compartment Jackfish cell was separated by a Nafion cation exchange membrane and filled with 0.1M KHCO$_3$. The bicarbonate electrolyte was prepared by saturating 0.05 M K$_2$CO$_3$ (Purity: 99.999%, American Elements) with CO$_2$ until the pH stabilized. The cell was installed in a Nicolet is50 FTIR equipped with a horizontally-configured VeeMAX III. The FTIR spectra were collected with a high-resolution MCT detector using p-polarized light and an angle of incidence of 75°. 20 scans were averaged at a resolution of 8 cm^{-1} to achieve a measurement time of 8 seconds per spectrum.

Results

The gold thin film was activated for SEIRAS by cycling in the CO$_2$-saturated 0.1M bicarbonate electrolyte (100 mV/s). The cyclovoltammetry limits were slowly increased from –0.4 to –0.7 V for the lower limit and 0.8 to 1.1 V for the upper limit to keep the current below 1 mA. The cycling was conducted until no further changes were detected in the current response (35 cycles, Figure
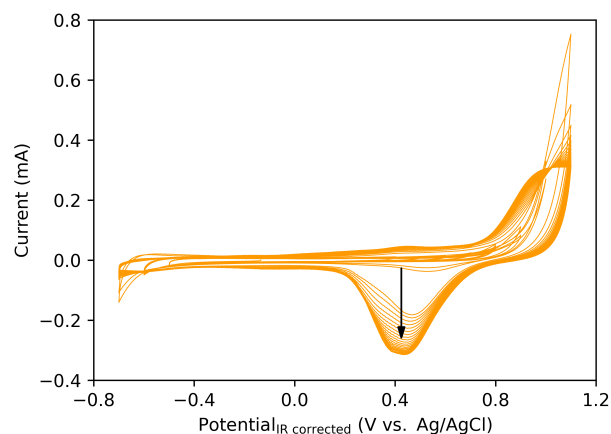
Figure 1a: Cyclic voltammetry of the as-prepared SEIRAS coating in CO$_2$-saturated 0.1M KHCO$_3$ electrolyte.
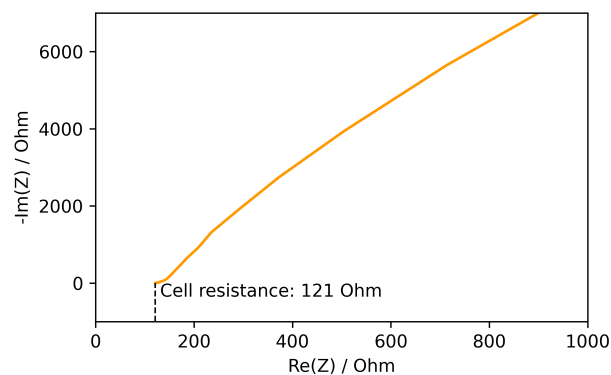
Figure 1b: Impedance measurement of the system in CO$_2$-saturated 0.1M KHCO$_3$.

1a). The impedance of the cell was measured to be ca. 121 Ohms and was in situ compensated to 85%.

To investigate the effect of stirring on eCO$_2$R, we conducted chronoamperometric measurements under CO$_2$ reduction conditions with and without stirring. Figure 2 shows the current response during eCO$_2$R at –0.6 V vs. RHE. Without stirring, the reaction current decreases over time, indicating a decrease in CO$_2$ reaction rate. In case of the stirrer being turned on, the current shows only a minor decrease of around 0.1 mA over the measurement period, demonstrating a stable reaction rate. The increase in noise in the measured current for the stirred measurement can be attributed to stirring-induced effects, such as moving bubbles disrupting the electrochemical interface, or electromagnetic interference from the stirring plate.
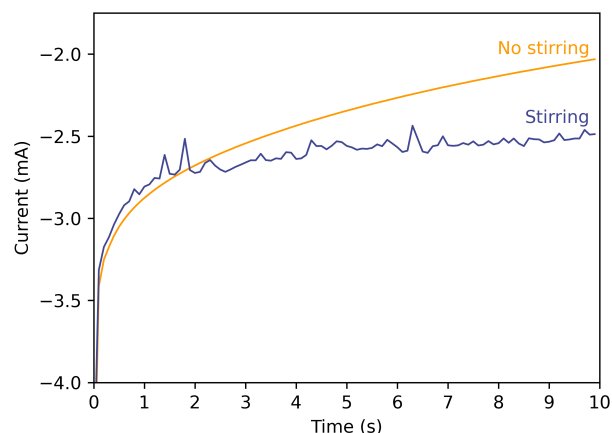
Figure 2: Current response during CO_2 reduction in 0.1M $KHCO_3$ at -0.6 V vs. RHE.
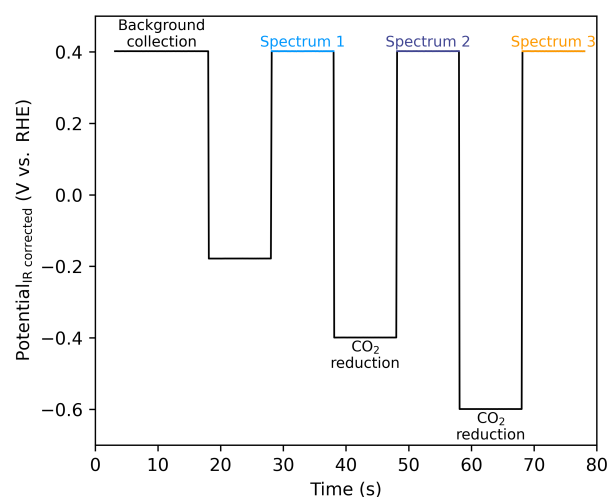
Figure 3: Measurement protocol to detect product accumulation at the working electrode.

We next tested the local reaction environment at the gold surface using a potential step technique developed by Dunwell and coworkers (Figure 3) [5]. Since CO is readily desorbed from the gold surface after formation, it cannot be detected under CO_2 reduction conditions. However, by stepping up the potential right after CO formation, the CO can be readsorbed on the Au surface, giving rise to the typical CO IR absorption band at around 2100 cm^{-1} [5]. Figures 4a and 4b show the resulting FTIR spectra of the stepped protocol in unstirred and stirred conditions. In the case of the non-stirred electrolyte, the FTIR spectrum shows a strong CO adsorption band at 2106 cm^{-1} after reduction at potentials < -0.4 V vs. RHE in accordance to the onset of CO_2 reduction. With decreasing potential, the intensity of the CO adsorption band increases and blueshifts to higher wavenumbers. Both intensity increase

and blueshift indicate a higher CO coverage on the Au surface. In contrast, the CO adsorption band is only weakly present under stirred conditions underlining the improved mass transport conditions that lead to quick CO removal after its formation. Furthermore, the unstirred system shows a decrease of dissolved CO_2 (peak at 2320 cm^{-1}) near the interface. Depletion of CO_2 can be related to consumption in eCO$_2$R but also local pH increase. Decreased CO_2 availability explains the diminished eCO$_2$R reaction currents in Figure 2. This demonstrates the crucial role that convection plays in SEIRAS measurements, especially when aiming to relate FTIR spectra to electrocatalytic performance measured in a different setup.
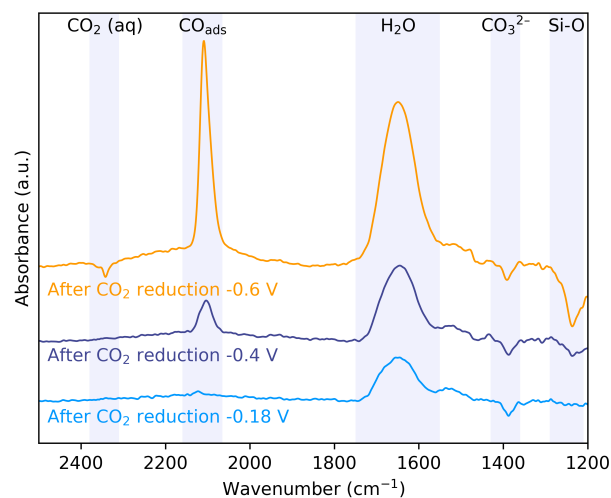
Figure 4a: FTIR spectra collected at 0.4 V vs. RHE after CO_2 reduction at the respective potential in the unstirred cell.
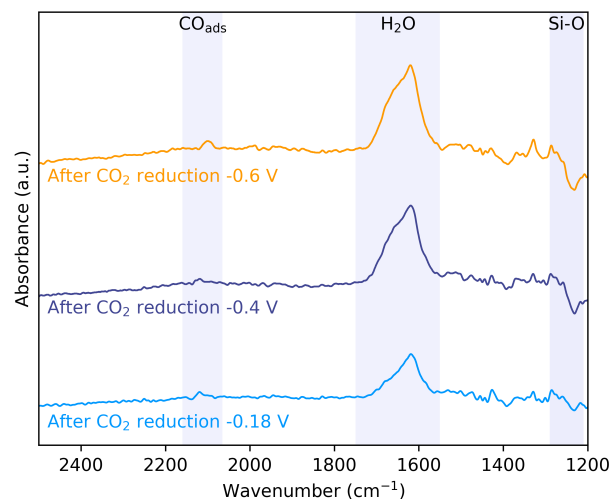
Figure 4b: FTIR spectra collected at 0.4 V vs. RHE after CO_2 reduction at the respective potential in the stirred cell.

References

(1) Yoo, J. M.; Ingenmey, J.; Salanne, M.; Lukatskaya, M. R. Anion Effect in Electrochemical CO_2 Reduction: From Spectators to Orchestrators. *J. Am. Chem. Soc.* **2024**, *146* (46), PMID: 39406354, 31768–31777, DOI: 10.1021/jacs.4c10661.

(2) Nitopi, S.; Bertheussen, E.; Scott, S. B.; Liu, X.; Engstfeld, A. K.; Horch, S.; Seger, B.; Stephens, I. E. L.; Chan, K.; Hahn, C.; Nørskov, J. K.; Jaramillo, T. F.; Chorkendorff, I. Progress and Perspectives of Electrochemical CO_2 Reduction on Copper in Aqueous Electrolyte. *Chem. Rev.* **2019**, *119* (12), PMID: 31117420, 7610–7672, DOI: 10.1021/acs.chemrev.8b00705.

(3) Chang, X.; Vijay, S.; Zhao, Y.; Oliveira, N. J.; Chan, K.; Xu, B. Understanding the Complementarities of Surface-Enhanced Infrared and Raman Spectroscopies in CO Adsorption and Electrochemical Reduction. *Nat. Commun.* **2022**, *13* (1), 2656, DOI: 10.1038/s41467-022-30262-2.

(4) Miyake, H.; Ye, S.; Osawa, M. Electroless Deposition of Gold Thin Films on Silicon for Surface-Enhanced Infrared Spectroelectrochemistry. *Electrochem. Commun.* **2002**, *4* (12), 973–977, DOI: 10.1016/S1388-2481(02)00510-6.

(5) Dunwell, M.; Lu, Q.; Heyes, J. M.; Rosen, J.; Chen, J. G.; Yan, Y.; Jiao, F.; Xu, B. The Central Role of Bicarbonate in the Electrochemical Reduction of Carbon Dioxide on Gold. *J. Am. Chem. Soc.* **2017**, *139* (10), 3774–3783, DOI: 10.1021/jacs.6b13287.